Stall-Flutter Analysis

Lars E. Ericsson* and J. Peter Reding†
Lockheed Missiles & Space Company Inc., Sunnyvale, Calif.

Dynamic stall and stall flutter, problems that have received a great deal of attention by the helicopter and compressor industry in the past, have recently become of great concern also to the aerospace industry because some of the winged space-shuttle vehicles will experience stall flutter in their transition from very high hypersonic entry angles to the substall angles of attack of the subsonic cruise portion of the reentry. Stall flutter is caused by the negative aerodynamic damping generated at stall penetration. An analysis is presented that can predict the stall-flutter boundaries, using static experimental data as an input. It is shown that the stall-flutter boundary measured in a subscale wind-tunnel test is representative of the true full-scale flutter boundary of a space-shuttle vehicle in its transition maneuver.

Nomenclature

a = speed of sound
AR = aspect ratio, $AR = b^2/S$
b = wing span
c,$\bar{c}$ = reference length: c = 2-D chord: $\bar{c} = S/b$
L = lift: coefficient $C_L = L/[(\rho_\infty U_\infty{}^2)/2]S$
l = section lift: coefficient $c_l = l/[(\rho_\infty U_\infty{}^2)2]c$
M = Mach number
M_p = pitching moment: coefficient $C_m = M_p/[(\rho_\infty U_\infty{}^2)/2]Sc$
m_p = section pitching moment: coefficient $c_m = m_p/\rho_\infty U_\infty{}^2/2)c^2$
p = static pressure: coefficient $C_p = (p - p_\infty)/(\rho_\infty U_\infty{}^2/2)$
R_c,$R_{\bar{c}}$= Reynolds number based on chord length
r_N = nose radius
S = reference area
S_0 = Strouhal number of cylinder wake shedding $S_0 = \bar{\omega}_0/2\pi$
t = time
U = velocity
V = flutter speed
v = velocity ratio, $v = U_e/U_\infty$
x = length coordinate along the chord
y = airfoil surface height
α = angle of attack
Δ = increment
η = dimensionless y-coordinate, $\eta = y/c$
θ = angle-of-attack perturbation
ξ = dimensionless x-coordinate, $\xi = x/c$
ρ = air density
ρ_N = nondimensional nose radius, $\rho_N = r_N/c$
ω = oscillation frequency
$\bar{\omega}$ = reduced frequency, $\bar{\omega} = \omega c/U$
$\bar{\omega}_0$ = reduced frequency of cylinder wake shedding, $\bar{\omega}_0 = \omega \times$ (diameter)$/U_\infty$

Subscripts

AM = apparent mass
e = boundary-layer edge conditions
N = nose
s = stall
SLE = shock-augmented leading-edge separation
STE = shock-augmented trailing-edge separation
∞ = undisturbed flow
1,2 = numbering subscript

Differential symbols

$\dot{\theta}$ = $\partial\theta/\partial t$
$\ddot{\alpha}$ = $\partial^2\alpha/\partial t^2$
$c_{l\alpha}$ = $\partial c_l/\partial\alpha$
v_ξ = $\partial v/\partial\xi$
$c_{m\dot{\theta}}$ = $\partial C_m/\partial\ c\dot{\theta}/U$
$c_{\bar{m}\dot{\theta}}$ = linear measure of nonlinear damping
i η' = $\partial\eta/\partial\xi$; $\eta'' = \partial^2\eta/\partial\xi^2$

Introduction

THE problem of stall flutter, which is of great concern to the helicopter and compressor industry, has recently become of significant interest to the aerospace industry. Some of the proposed space-shuttle configurations have wings that will be subject to stall flutter at some time period during the transition maneuver from very high hypersonic entry angles to substall angles of attack for subsonic cruise.[1]

The problem of stall flutter,[2,3] like that of launch vehicle buffet,[4,5] is caused by separated-flow-induced negative damping and is not usually the result of resonance between structural oscillations and dominant harmonics in the aerodynamic forcing function. The forcing function is present and is important, but stall flutter cannot be eliminated by avoiding a critical structural frequency or staying away from the vehicle velocity giving the resonant (reduced) aerodynamic frequency (the critical Strouhal number). Stall flutter is present at all frequencies where negative aerodynamic damping exists. It can only be eliminated by decreasing the negative aerodynamic damping until it is less in magnitude than the structural damping. Usually, this balance is obtained only after the oscillations have reached a limit cycle amplitude, in which case the structure dissipates energy at the same rate as the surrounding airstream delivers energy to the airfoil.

Because of the complexity of the stall-flutter problem, almost all contributions toward an understanding of the phenomenon have been the result of systematic experimental investigations. Since the classical investigation by Halfman et al.[6] "two-dimensional" unsteady airfoil stall has received much attention.[7-9] However, even the results of dynamically scaled model tests may not be applicable to full-scale flight because of interference effects from model supports and wind-tunnel walls or side plates.[10] The alternative approach, testing a subscale model of an actual component (e.g., a helicopter rotor), involves the usual Reynolds number scaling problem as well as wall interference effects. Where detailed instrumentation is used, however, valuable information can be obtained about airfoil stall without end-plate effects.[11-13]

Presented as Paper 72-380 at the AIAA/ASME/SAE 13th Structures, Structural Dynamics, and Materials Conference, San Antonio, Texas, April 10-12, 1972; submitted April 17, 1972; revision received October 12, 1972. The results presented in this paper were obtained in a study performed for the NASA-Langley Research Center (Contract NAS 1-9987) under direction of P. Hanson.

Index categories: Nonsteady Aerodynamics; Structural Dynamic Analysis; Airplane and Component Aerodynamics.

*Senior Staff Engineer. Associate Fellow AIAA.
†Research Specialist. Member AIAA.

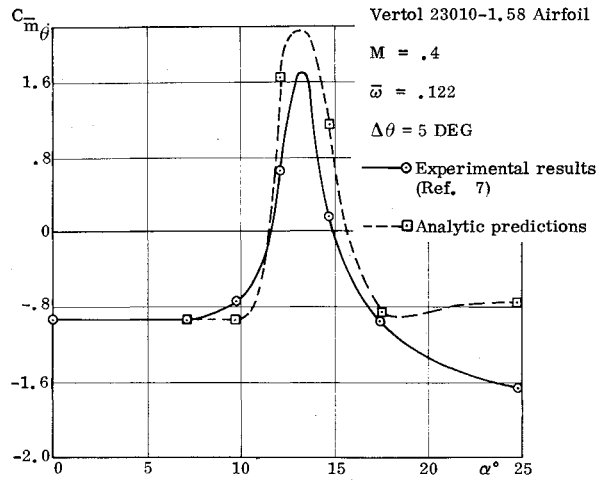

Fig. 1 Predicted and measured pitch damping at low frequency.

It is clear that neither test nor theory alone will provide a satisfactory solution, at least not in the near future. This situation is likely to prevail even when considering the recent resurgence of theoretical attacks on the dynamic stall problem.[12,14,15] The only realistic approach is to combine theory and experiments to provide the capability for prediction of dynamic stall and stall flutter. The standard approach has been to use dynamic experimental data to provide a semiempirical theory.[1,2,6,8,16-18] The disadvantage with this approach is that the method is very configuration-dependent and requires dynamic test data which are always expensive to obtain and not always reliable to use.[10]

This paper presents an alternative approach. The unsteady aerodynamic characteristics are related theoretically to static aerodynamic characteristics. Static experimental data are readily available for a great number of airfoil shapes, and new data, if needed, are relatively cheap to obtain. Preliminary results show good agreement with experimental dynamic stall data.[19] The analysis has since then been extended to higher frequencies and to include compressibility effects.[20] This analysis is applied here to determine the boundaries for stall flutter, in particular for the straight wing of one candidate space-shuttle configuration.[1]

Analysis

The two flow phenomena that cause stall flutter are 1) a dynamic overshoot of static stall and undershoot of static reattachment loads, and 2) an additional lag of the deep stall airloads over and above the attached flow Karman-Sears vortex-wake-lag.[21] The overshoot is the result of pressure-gradient lag and dynamic improvements of the boundary-layer shape parameter upstream of separation.[20] The additional deep-stall lag effect is generated by the separation point velocity relative to the airfoil surface.[20,22] The analytic theory for prediction of the nonlinear unsteady characteristics of an airfoil penetrating the stall region at finite oscillatory amplitudes is presented elsewhere.[23] An example of agreement between the experimentally observed[7] and predicted[23] negative damping is shown in Fig. 1. It can be seen that the damping derivative varies very steeply with α at the stall-flutter boundary, $C_{\bar{m}\dot{\theta}} = 0$, for pitch oscillations of 5° amplitude. It therefore would be expected that the stall-flutter boundary for finite amplitudes is not much different from that for infinitesimal amplitudes. This expectation is confirmed by experimental results,[24] and also by theoretical arguments, as will be shown later. The stall-flutter boundary is determined by using static experimental data in combination with theoretical arguments.

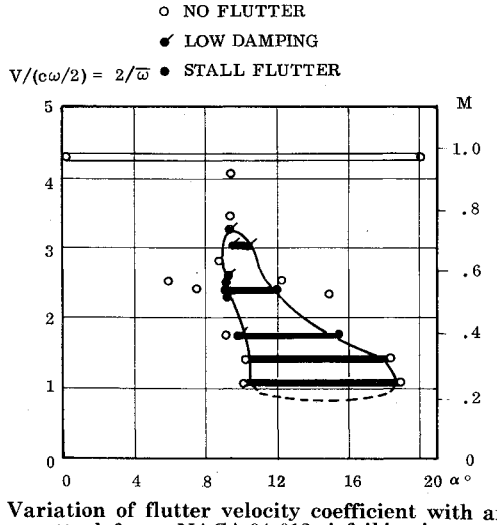

Fig. 2 Variation of flutter velocity coefficient with angle of attack for an NACA 64-012 airfoil in air.

Stall-Flutter Boundary

The stall-flutter boundary for a space-shuttle wing concept determined by wind-tunnel tests of an elastic model[25] is shown in Fig. 2. The stall-flutter region consists of high- and low-angle-of-attack boundaries. It disappears at high-Mach-number/low-reduced-frequencies and has also a low-Mach-number/high-reduced-frequency cutoff.

The high and low α-boundaries are determined by the dynamic overshoot of static stall and undershoot of static reattachment, respectively. The high α-limit is simply the highest α at which an airfoil describing torsional oscillations of high frequency and small amplitude will have attached flow on the "upstroke"; that is, the highest α at which the dynamic boundary-layer improvements are large enough to produce attached flow. Conversely, the low α-limit is the lowest α at which the airfoil can get separated flow on the "downstroke." The high-Mach-number cutoff is a compressibility effect, and the low-Mach-number/high-reduced-frequency cutoff is caused by wake-shedding phenomena.

Dynamic $C_{L\max}$

Substantial overshoot of static $C_{L\max}$ has been observed on aircraft penetrating the stall region at non-zero pitch-up rate, as shown in Fig. 3.[26] The figure shows that the overshoot slopes $\partial C_{L\max}/\partial(c\dot{\alpha}/U_\infty)$ are essentially invariant with Mach number and/or Reynolds number. Figure 3 also indicates that there is an upper limit for the dynamic over-shoot of the static $C_{L\max}$. It will be shown that this limit, which is designated $(C_{L\max})_{\text{limit}}$ determines the upper boundary $\alpha_{s\max}$ for stall flutter.‡ The third important feature presented in Fig. 3 is the drastic change of $(C_{L\max})_{\text{limit}}$ with Mach number and/or Reynolds number. It will be shown that this is mainly a Mach number effect, and is providing the high-Mach-number/low-frequency cutoff of the flutter region.

Several reasons can be given for the dynamic overshoot of static stall.[19,20] The dominant reason is the favorable influence on boundary-layer thickness and shape parameter of pressure gradient lag and "moving wall" effects. The moving wall velocity induced by the pitch rate is negligibly small everywhere but at the leading edge.[20] However, the decelerating wall velocity around the leading edge generates a wall-jet-like effect (see Fig. 4). When the

‡This α-overshoot limit, determined from C_L-characteristics, is assumed to be valid also for the C_m-characteristics.

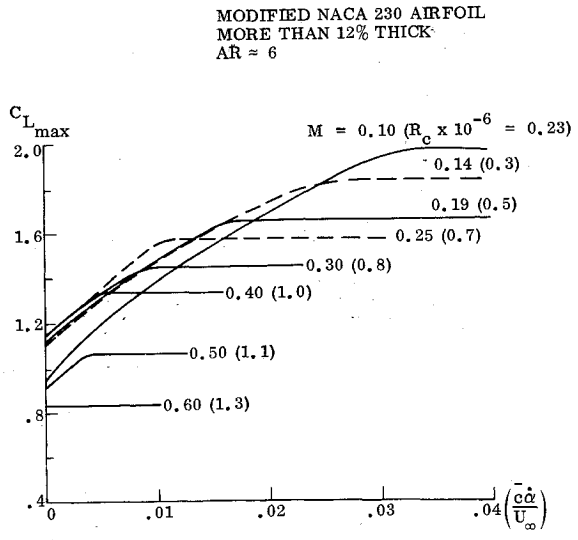

Fig. 3 Dynamic stall and $C_{L\max}$ overshoot.

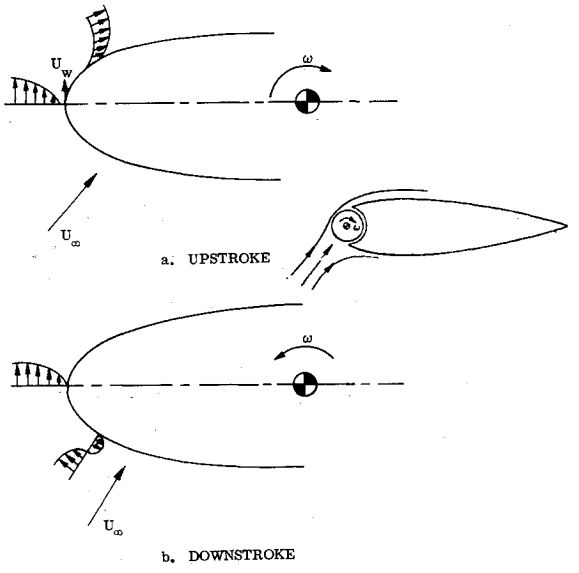

Fig. 4 Pitch-rate-induced decelerating wall effect.

flow rounds the corner to the upper surface of the airfoil, the tangential velocity of the wall decreases very rapidly and the near-wall boundary layer is left with an excess velocity, strengthening the boundary layer, as is indicated in Fig. 4a. On the downstroke, the leading edge accelerates the flow downward, causing a separation-prone boundary-layer shape change (see Fig. 4b).

There is no experimental data available to prove or disprove this hypothesis. A test of an airfoil with a rotating cylinder as the leading edge (see inset in Fig. 4) could answer this question. The results obtained by Wallis,[27] using blowing on the windward side of the airfoil (between stagnation point and leading edge), tends to lend some support to this hypothesis. However, Wallis' objective was to generate small-scale vortices to increase the turbulence in the boundary layer and thereby simulate an increase of Reynolds number. The dynamic leading edge effect may also be one of vortex generation, and it is likely to be even more complex than that. A detailed answer to this question is not needed for the present analysis. The dynamic leading edge wall-jet-like effect sketched in Fig. 4 is conceptually very appealing, but any other mechanism producing similar characteristics would do; i.e., the dynamic boundary-layer effects are 1) reversible (that is, the effects are opposite on the "downstroke" to what they are on the "upstroke") and 2) proportional to the dimensionless angular rate, $c\dot{\alpha}/U_\infty$, at least to first-order accuracy. The inviscid pressure gradient lag effect[14] over and above the Karman-Sears vortex-wake lag effect[21] is negligible in itself.[23] However, its influence on boundary-layer shape parameter and thickness, as determined by a quasi-steady Karman-Pohlhausen-type analysis,[28] may not be negligible. This effect would also have the postulated characteristics (reversibility and pitch rate proportionality), and would be somewhat equivalent to a Reynolds number change.

The linear dependence of the $C_{L\max}$-overshoot on the pitch rate, $c\dot{\alpha}/U$, is displayed by the experimental data in Fig. 3. In regard to $(C_{L\max})_{\text{limit}}$, the "ceiling" in Fig. 3, Wallis' results[27] suggest that it should correspond to the limit of static $C_{L\max}$ for infinitely large Reynolds numbers, $(C_{L\max})_{Rc\to\infty}$. This limit should be obtained on an airfoil reshaped in regard to nose-droop and surface curvature according to the beneficial dynamic pressure-gradient effect. It appears that when the full beneficial Reynolds number effects are realized, $C_{L\max} = (C_{L\max})_{Rc\to\infty}$, the shape change effects have also reached their limit. It is true that the ceilings in Fig. 3, which reflect the data-interpretations by Harper and Flanigan,[26] could be given a very slight inclination with increasing $c\dot{\alpha}/U_\infty$. This would correlate better with the actual data points, which scatter around this fairing as much as $\Delta C_L = \pm 0.1$. However, this slope is accounted for in its entirety by apparent-mass effects; the quasi-steady $(C_{L\max})_{\text{limit}}$ is the one shown in Fig. 3.

The only dynamic effects not represented in the above quasi-steady similitude approach are the transient loads. The apparent mass effect is as follows:

$$(\Delta c_l)_{AM} = (C_{L\dot{\alpha}})_{AM}(c\dot{\alpha}/U_\infty) = c_{l\alpha}[(c_{l\dot{\alpha}})_{AM}/c_{l\alpha}](c\dot{\alpha}/U_\infty) \quad (1)$$

Thin airfoil theory gives $(\Delta c_l)_{AM} = 0.25\, c_{l\alpha}(c\dot{\alpha}/U_\infty)$: That is, for the pitch rates of interest here, $c\dot{\alpha}/U_\infty < 0.05$, the contribution from apparent mass effects to $c_{l\max}$ is

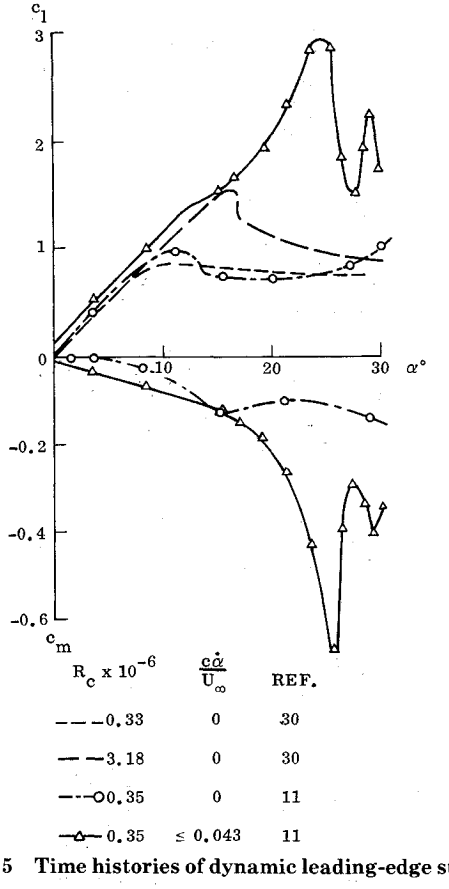

Fig. 5 Time histories of dynamic leading-edge stall.

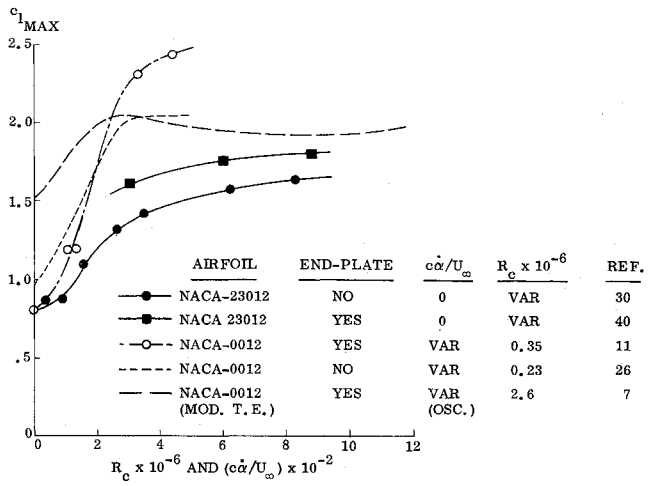

Fig. 6 $c_{l\max}$ as a function of R_c and $c\dot{\alpha}/U_\infty$.

$(\Delta c_l)_{AM} < 0.1$, well within the scatter of the $(c_{l\max})_{\text{limit}}$ data.

More important is the transient lift generated by a "spilled" leading-edge vortex[11,29] or an elongating separation bubble.[15] The test results obtained by Ham and Garelick[11] vividly illustrate this transient lift production (see Fig. 5). The oscillatory behavior at peak c_l is explained by the "spilled vortex" travel over the airfoil chord.[13,29] However, even disregarding the c_l-oscillation, the overshoot of static $c_{l\max}$ is larger than expected. There are several explanations for this "super-overshoot" of static $c_{l\max}$. For high $(c\dot{\alpha}/U)$-values, the value of $c^2\ddot{\alpha}/U^2$ becomes important.[20,23] Increasing $\dot{\alpha}$ during the overshoot of the static stall angle α_s delays the movement forward of the separation point to the full deep-stall position, thus generating extra lift. In the oscillatory case, the overshoot of α_s will always occur with a decreasing $\dot{\alpha}$-rate; i.e., no such super-overshoot is expected. A point of some concern is that the test Reynolds number is such that the static stall should be of the laminar trailing edge type[30] and that the Ham-Garelick static data show a peculiar overshoot of these laminar stall characteristics. Although Ham and Garelick seem to have been rather careful to avoid most of the pitfalls associated with so-called "two-dimensional" stall tests,[10] this overshoot already at $c\dot{\alpha}/U = 0$ creates some uncertainty about the true cause of the super-overshoot at high $c\dot{\alpha}/U$. The use of a row of pressure orifices in combination with endplates can possibly produce a distorted view of dynamic two-dimensional stall, even for large-span models.[10]

Since the presentation of the above speculations,§ some readers have questioned the advisability of publishing such speculations without more supporting data. The MIT research under the direction of Ham has provided industry with fundamental new knowledge about the dynamic stall process. Because the results are so fundamental and are used so widely, the present authors felt that it was important to bring into the discussion everything that could help explain this "super-overshoot." There is now data available that supports our speculations.[31,32] ¶Moss and Murdin[31] found that their NACA 0012 "two-dimensional" wing (with span-to-chord ratio of 3.75; the effective** ratio for Ham et al. is 4.8) had a midspan stall-cell that was "vented" through a horseshoe vortex. Gregory et al.[32] continued to investigate in more detail this separated flow phenomenon. They concluded that not only is the flow taking on a three-dimensional character when there is an appreciable extent of separated flow, but boundary-layer control applied in the corners at the ends of the airfoil, as has been used by Liiva et al.,[7] for example, does not necessarily inhibit the development of three-dimensionality even when it extinguishes the separation in the airfoil-endplate corner (The investigated span-to-chord ratios ranged from 1.28 to 2.8).

McCroskey, and Fisher[13] found in their detailed measurements of dynamic stall on a subscale model of a helicopter rotor that 1) the pressure distribution at stall varied in a manner that would be explained by a "spilled" leading edge vortex, and 2) the large sectional normal force measured at dynamic stall on the rotor blade correlated rather well with that measured by Ham and Garelick.[11] That is, the "two-dimensional" test[11] provided a fairly good simulation of three-dimensional dynamic stall on a helicopter blade.[13] According to the ideas put forth in the present paper (and in Ref. 23), the reason for the correlation of this "super-overshoot" is a similarity in the "non-two-dimensional" steady-state flowfields, and not a similarity between basically two-dimensional unsteady airfoil stall characteristics as has been assumed before by most researchers, including the present authors.[29] McCroskey and Fisher showed that the "super-overshoot" could indeed be explained by static three-dimensional flow effects (Fig. 15 of Ref. 13). If full-scale experimental static data was used, the large normal force overshoot in the subscale dynamic model test (at an order-of-magnitude lower Reynolds number) could be predicted using the unsteady semiempirical theory based on oscillatory stall measurements.[7] This result supports the dynamic leading edge effect—infinite Reynolds number similarity proposed in the present paper. We suggest, therefore, that the agreement between the Ham-Garelick two-dimensional test data and the three-dimensional section characteristics measured by McCroskey and Fisher could be fortuitous; that is, the reason for the similarity could be that in the Ham-Garelick test the wing-side wall horseshoe vortex described by Moss and Murdin[31] supplied venting of the separated flow region in a manner similar to the venting provided by the tip vortex from the rotor blade in the McCroskey-Fisher test.

When static $c_{l\max}$ vs Reynolds number is plotted,[30,33] together with dynamic $c_{l\max}$ versus pitch rate $(c\dot{\alpha}/U)$,[11,26] it is again found that the Ham-Garelick data overshoot the results from other tests (see Fig. 6). The $c_{l\max}$ data obtained by Liiva et al.[7] in pitch oscillation tests seem to "level out" at the same level as the corresponding endplated static data for $R_c \to \infty$. This limit is reached already at $c\dot{\alpha}/U = 0.2$, for both rampwise and oscillatory change of pitch rate. That means that the limit in oscillatory tests is reached at the amplitude $\Delta\theta = 0.2/\bar{\omega} \approx (\bar{\omega})^{-1}$ deg. As $\bar{\omega}$ typically is larger than unity in a flutter test[25] (see Fig. 2), the infinite Reynolds number limit is approached already for amplitudes below $\Delta\theta = 1°$. Thus, one can assume the dynamic overshoot in a flutter test to be the maximum possible; i.e.,

$$(c_{l\max})_{\text{dyn}} = (c_{l\max})_{\text{limit}} = (c_{l\max})_{R_c \to \infty} \qquad (2)$$

Figure 3 shows that this limit is quite sensitive to Mach number.

Effect of Compressibility on $(c_{l\max})_{\text{limit}}$

At first glance, the data in Fig. 3 indicate that the different $(C_{L\max})_{\text{limit}}$-values for $M < 0.4$ are caused by Reynolds number variation, rather than compressibility effects. Although the assumption of incompressible flow

§AIAA/ASME/SAE 13th Structures, Structural Dynamics, and Materials Conference, San Antonio, Texas, April 10–12, 1972.

¶The reports were available already in 1969 and 1970 in the form of RAE Technical Report 68104 and NPL Aero Report 1309. However, the present authors' literature research did not uncover them.

**The span-to-chord ratio is 8.4, but the chord-wise pressure distribution was measured at 43% of semispan and not in the midspan section.

results for $M < 0.4$ usually is good, it is completely false in the case of stall data. The peak velocity on the airfoil at stall angles of attack is several times higher than at $\alpha = 0$. Using the simple analysis by Ville,[34] one can determine the compressibility effects as follows: Near the leading edge, all NACA airfoil shapes are well approximated by a parabola, with the nose radius as the characteristic length

$$\eta^2 = 2\rho_N \xi \tag{3}$$

The velocity determined by potential flow theory is as follows for moderate α[33,34]

$$v = U_e/U_\infty = \{\xi^{0.5} + [1 + (\rho_N/2)^{0.5}]\alpha\}/(\xi + \rho_N/2)^{0.5} \tag{4}$$

$$v_\xi = \partial v/\partial\xi = \{(\rho_N/2)\xi^{-0.5} - [1 + (\rho_N/2)^{0.5}]\alpha\}/2(\xi + \rho_N/2)^{1.5} \tag{5}$$

From Eqs. (4) and (5) one obtains

$$(U_e/U_\infty)_{\max} = \{1 + [1 + (\rho_N/2)^{0.5}]^2 \alpha^2/(\rho_N/2)\}^{0.5} \tag{6}$$

The effect of angle of attack on peak velocity ratio, as defined by Eq. (6), is illustrated in Fig. 7 for the ($\rho_N - \alpha$) range of interest. For a typical nose radius (e.g., ρ_N = 1%), the tunnel Mach number at $\alpha = 10°$ would have to be $M_\infty \leq 0.1$ in order to correspond to the low angle-of-attack assumption for incompressibility; i.e., $M_e \leq 0.4$. Thus, for all practical purposes there is no such thing as incompressible airfoil stall. Unfortunately, for most of the available static stall data, there is no information available for test Mach number. The range usually given is 150 mph $\leq U_\infty \leq$ 300 mph. This corresponds to $0.2 \leq M_\infty \leq 0.4$. This Mach number range can cause quite a change in $(C_{L\max})_{\text{limit}}$, as is shown in Fig. 3.

In using static experimental data to define the stall-flutter boundaries, it is apparent from the above discussion that a crucial portion of that task is to be able to predict the effects of compressibility on dynamic overshoot of static stall.

The effect of surface slope or thickness is scaled by the Prandtl-Glauert Analogy[35]

$$\eta' = \frac{\partial\eta}{\partial\xi} \cdot (1 - M_\infty^2)^{0.5} \tag{7}$$

This is all right for a sharp leading-edge airfoil at low α, when maximum velocity is determined by airfoil thickness. However, on a "round-nosed" airfoil at stall, the maximum velocity occurs at the nose, and surface curvature rather than slope determines the peak velocity. Following the usual procedure—i.e., neglecting the effect of η' compared to η'' when determining the curvature—suggests that near stall, the peak velocity, and hence the flow separation, is scaled by η''. Equations (3) and (7) give

$$\eta'' = -\eta'^3/\rho_N \cdot (1 - M_\infty^2)^{1.5} \tag{8}$$

That is,

$$[(c_{l\max})_2/(c_{l\max})_1]_{R_c \to \infty} = [(1 - M_2^2)/(1 - M_1^2)]^{1.5} \tag{9}$$

The $(C_{L\max})_{\text{limit}}$ data[26] in Fig. 3 and data from a flight test[36] are shown in Fig. 8 as functions of Mach number. Also shown is the static $(C_{L\max})_{Rc \to \infty}$ as obtained trom Fig. 6 for the finite-aspect ratio wing (without endplate). The agreement between the extrapolation from static data using Eq. (9) is surprisingly good. The Mach number spread reflects the uncertainty given in Ref. 30; i.e., 150 mph $\leq U_\infty \leq$ 300 mph. The low limit gives very good agreement with the dynamic data. It is probable that the low tunnel velocity would have been used for the $C_{L\max}$ runs due to balance and model load considerations. The flight-test data are offset from the wind tunnel data. This could simply be an indication of a bias error in the flight instrumentation vis-à-vis the tunnel balance in determining $C_{L\max}$. Still, the agreement between flight data and wind tunnel data is very encouraging, considering the order-of-magnitude difference in Reynolds number; that is, the hypothesis that Reynolds number is insignificant for $(C_{L\max})_{\text{limit}}$ seems to be a good first approximation.

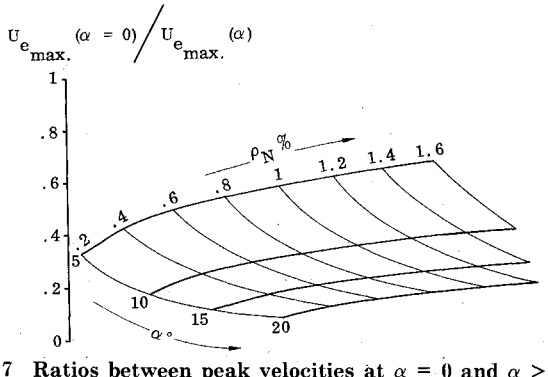

Fig. 7 Ratios between peak velocities at $\alpha = 0$ and $\alpha > 0$ as function of nose radius and angle of attack.

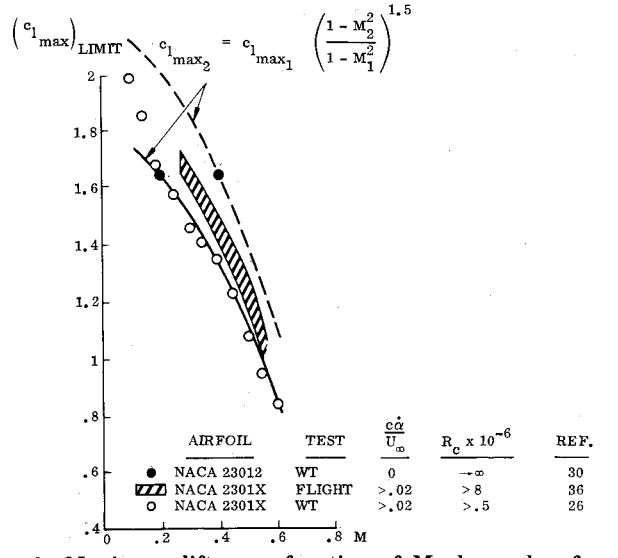

Fig. 8 Maximum lift as a function of Mach number for a NACA-230XX airfoil.

Dynamic Reattachment $c_{l\min}$

As the dynamic effects on the downstroke are opposite to what they are on the upstroke, it could be expected that the lift at reattachment would approach the limit for static $c_{l\max}$ when the Reynolds number approaches zero; that is,

$$c_{l\min} = (c_{l\max})_{R_c \to 0} \tag{10}$$

Using part of Fig. 6, and adding more of Liiva's data,[7] gives the results shown in Fig. 9. It appears that Liiva's $c_{l\min}$ for oscillatory reattachment approaches qualitatively the zero Reynolds number limit for static $c_{l\max}$. An obvious reason†† cannot be found for the undershoot of this limit for pitch rates in the range $0.2 < c\dot{\alpha}/U_\infty < 0.08$. The dynamic data in Fig. 9 are for $M \leq 0.4$. As before, for

††The data in Ref. 32 suggest that differences in model test set-up, such as the corner blowing used by Liiva[17] but not by Abbot et al.,[33] could account for at least part of this deviation.

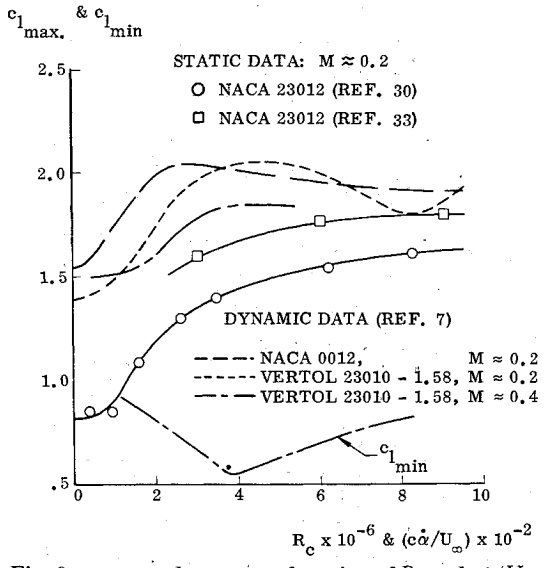

Fig. 9 $c_{l\max}$ **and** $c_{l\min}$ **as a function of** R_c **and** $c\dot{\alpha}/U$.

$(c_{l\max})_{Rc\to\infty}$, it will be necessary to account for compressibility effects in regard to $(c_{l\max})_{Rc\to\infty}$.

The zero Reynolds number limit for $c_{l\max}$ implies that the separation is fixed, and nose curvature is no longer important. One would expect that the sharp-leading-edge/thickness-dominated case, Eq. (7), is the appropriate scaling model. Thus

$$[(c_{l\max})_2/(c_{l\max})_1]_{R_c\to 0} = [(1-M_2^2)/(1-M_1^2)]^{0.5} \quad (11)$$

Flight-test data[37] for a thick wing in pull-up maneuvers gives some indication of the appropriateness of Eq. (12). The flight-test data show also another feature, viz., an inflection point in the $c_{l\max}(M)$-curves. At higher Mach numbers, the M-dependence given by Eq. (9) is obviously not valid. When the leading-edge stall is shock induced, the effect of Mach number on $c_{l\max}$ becomes much less. Tests indicate that the $c_{l\max}(M)$-dependence is the same for rounded leading-edge airfoils as for double circular-arc airfoils.[38] This insensitivity to geometry has also been demonstrated for other airfoils. Thus, the maximum lift is

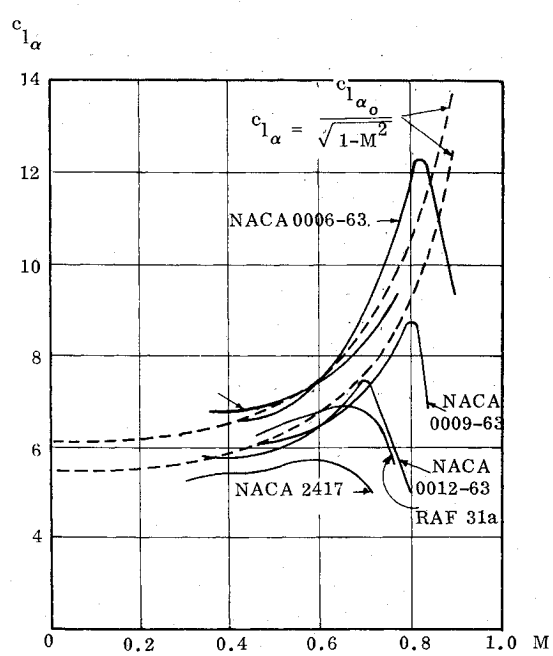

Fig. 10 Effect of Mach number on lift-curve slope.

determined by the airfoil thickness, and Eq. (11) applies for $M_{SLE} < M < M_{STE}$. The critical Mach number M_{SLE} is that giving shock-augmented leading-edge separation. For Mach numbers above M_{STE}, the shock is moving back towards the trailing edge, and the separation is of the shock-augmented trailing-edge type.

It is obviously important to determine M_{SLE} for the particular airfoil of interest. Pearcy[39] shows that incipient separation occurs when the shock strength is $p_2/p_1 \approx 1.4$, and that full, shock-augmented, leading-edge separation occurs when the local Mach number approaches $M_e = 1.4$ (slightly lower M_e for thinner airfoils than 12%). The corresponding M_∞ is determined as follows: Determine $U_{e\max}(\alpha_0)/U_\infty$, where α_0 is the angle of attack, giving "flat-top" velocity distribution over the airfoil.[33] Determine $U_{e\max}(0)/U_{e\max}(\alpha_0)$ and $U_{e\max}(0)/U_{e\max}(\alpha_s)$ from Fig. 7. Thus

$$\frac{U_{e\max}(\alpha_s)}{U_\infty} = \left[\frac{U_{e\max}(0)}{U_{e\max}(\alpha_o)} \Big/ \frac{U_{e\max}(0)}{U_{e\max}(\alpha_s)}\right] \frac{U_{e\max}(\alpha_o)}{U_\infty} \quad (12)$$

For $M_e = 1.4$, the Mach number ratio corresponding to Eq. (12) is simply

$$M_{e\max}(\alpha_s)/M_\infty = [U_{e\max}(\alpha_s)/U_\infty]/0.85 \quad (13)$$

For the thick airfoil, a value of $M_{SLE} = 0.30$ is obtained. For the airfoil used in the stall-flutter test,[25] NACA 64-012, the value is $M_{SLE} = 0.35$.

In summary, then, the compressibility effects on the maximum lift are given by Eq. (9) when $M < M_{SLE}$, and by Eq. (11) when $M \geq M_{SLE}$. The reattachment lift $c_{l\min}$ is always obeying Eq. (11).

Dynamic Stall and Reattachment Angles of Attack

For the Mach number range $M \leq 0.6$, the lift curve slope variation with Mach number is predicted by the Prandtl-Glauert compressibility factor[35] (see Fig. 10).

$$(c_{l\alpha})_2/(c_{l\alpha})_1 = [(1-M_1^2)/(1-M_2^2)]^{0.5} \quad (14)$$

Figure 10 shows that there is a dramatic decrease in $c_{l\alpha}$ for higher Mach numbers, (e.g., at $M > 0.7$ for NACA 0012-63.[40] It is likely that this critical Mach number is simply $M = M_{STE}$, as previously discussed.‡‡ The finite-aspect ratio (AR) lift curve slope is simply:

$$C_{L\alpha} = c_{l\alpha}/(1 + c_{l\alpha}/\pi AR) \quad (15)$$

With the linear relationship: $c_{l\max} = c_{l\alpha}\alpha_s$, one obtains the following definition of the stall angle of attack α_s

$$\left.\begin{aligned} (\alpha_{s2}/\alpha_{s1})_{R_c\to\infty} &= [(1-M_2^2)/(1-M_1^2)]^2 \\ M &< M_{SLE} \\ (\alpha_{s2}/\alpha_{s1})_{R_c\to\infty} &= (\alpha_{s2}/\alpha_{s1})_{R_c\to 0} \\ M_{SLE} < M < M_{STE} \qquad & M < M_{STE} \\ &= (1-M_2^2)/(1-M_1^2) \end{aligned}\right\} \quad (16)$$

Prediction of Stall-Flutter Boundaries

Stall flutter is the result of the negative aerodynamic damping that occurs when stall is penetrated, as was discussed earlier. The high and low α-boundaries for stall flutter have been shown to be simply $\alpha_{\max} = (\alpha_s)_{Rc\to\infty}$

‡‡An increase in $c_{l\max}$[38] compensates partially for this loss when considering α_s.

and $\alpha_{min} = (\alpha_s)_{Re\to 0}$. There is, of course, a strong relationship between the static α-M stall boundary and the low α-M boundary for stall flutter. It is a realistic boundary for stall flutter as occurring for increasing angles of attack. However, for the space-shuttle transition maneuver,[41] where the angle of attack is continually decreasing, such a boundary is not realistic according to the present study. The wing is in deep stall initially, and stall flutter starts when the angle of attack is decreased below the highest value for which reattached flow can be established on the upstroke. Stall flutter will persist as long as detached flow can be realized on the down-stroke. Due to the high reduced frequencies associated with stall flutter of a wing, these high and low α-boundaries for stall flutter will be close to the static stall limits for infinite and zero Reynolds number discussed earlier. The stall flutter α-boundaries determined in this manner for the NACA 64-012 airfoil tested by Goetz[25] are shown in Fig. 11. The low α-boundary is conservative because of the way the static-stall angle for low R_c was determined (see inset in Fig. 11). At $M = 0.7$, the $c_{l\alpha}$-slope changes drastically for a 12%-thick airfoil, (Fig. 10), thus indicating that $M_{STE} = 0.7$; i.e., the shock starts moving aft over the airfoil for increasing M. The α = constant line for $M > M_{STE}$ agrees with the combined effect of $c_{l\alpha}$-loss and $c_{l\max}$-increase for increasing Mach number. At some Mach number between $M = 0.8$ and $M = 0.9$, the shock has moved aft of the elastic axis, or nearly so (the flutter model had 5% structural damping), and flutter is not observed. In other words, this high-Mach-number/low-frequency cutoff of the flutter boundary is a pure Mach number effect, independent of reduced frequency but somewhat dependent upon elastic axis location and structural damping.

The flutter boundary also has a low-Mach-number/high-frequency cutoff. It has been speculated that this is a combined effect of Mach number and reduced frequency and that the scaling parameter for this effect is the product $M\bar{\omega} = c\omega/a$. As Freon-12 has half the sonic speed of air, test in Freon made it possible to increase this parameter enough to demonstrate the low M cutoff[25] (see Fig. 12). There is a rule of thumb for this cutoff: "No flutter for $c\omega/a > 1''$—a criterion that has been proposed by

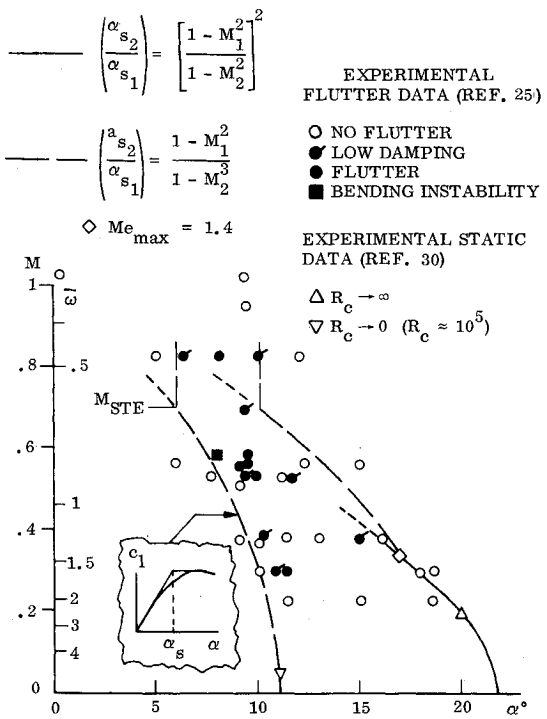

Fig. 11 Predicted and measured boundaries for stall flutter.

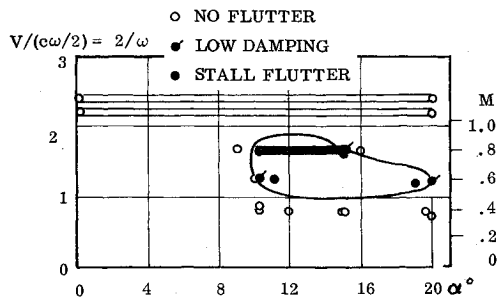

Fig. 12 Variation of flutter velocity coefficient with angle of attack for an NACA 64-012 airfoil in Freon 12.

Baker.[42] However, there are more realistic explanations for this low-M/high-$\bar{\omega}$ cutoff.

Comparing Figs. 2 and 12, one notices that the flutter boundary in both cases is cut off at $\bar{\omega} \geq 2$. At high reduced frequencies one expects that the natural shedding of von Kármán-type vortices will enter into the problem. The "dual sheet" Karman vortex shedding from an airfoil with spoiler will respond with the frequency $\bar{\omega}_w$ to airfoil oscillations at frequency $\bar{\omega}$, where $\bar{\omega}_w$ is determined as follows.[43]

$$\bar{\omega}_w = (1 + \xi_s^{0.5}/2)^2\, \bar{\omega}_o \tag{17}$$

At stall, the top side separation point moves to the leading edge, $\xi_s = 0$, and $\bar{\omega}_w = \omega_0/4$. Using the equivalent cylinder diameter, $c \sin \alpha_s$, one obtains $\bar{\omega}_0 = 2\pi S_0/\sin \alpha_s$ where $S_0 \approx 0.2$. With $\alpha_s \leq 19°$, $\bar{\omega}_w \geq 1$. If, instead, the Karman vortex shedding frequency set by the distance between separation point, $\xi_s = 0$, and training edge, $\xi = 1$, is considered, exactly half the regular cylinder shedding frequency is obtained—i.e., $\bar{\omega}_w = \bar{\omega}_0/2$. This value is in good agreement with recent results obtained by Scruggs.[44] For $12° < \alpha_s \leq 19°$, $\bar{\omega}_w$ is as follows: $2 \leq \bar{\omega}_w < 3$; that is, the following frequency range for the Karman vortex shedding from an airfoil in (deep) stall is suggested:

$$1 < \bar{\omega}_w < 3 \tag{18}$$

This is in the right range for the high-frequency cutoff of the stall flutter boundary (Figs. 2 and 12), but the question of the cause of the cutoff remains. With the separation point ξ_s free, rather than fixed, there is a mechanism for initial overshoot and associated motion-dependence of the frequency and amplitude of the vortex-wake-oscillation. It has been shown by Parkinson[45] that the Karman vortex shedding off circular cylinders can be both amplitude and frequency modulated (up to 40%) by oscillating the cylinder normal to the incoming flow. Scruggs has obtained similar results both for cylinders and airfoils;[44] that is, when the airfoil oscillation frequency is close to the wake frequency, strong coupling effects can be expected. This phenomenon has indeed been demonstrated. Cincotta, Jones, and Walker observed that the vortex wake damped the cylinder oscillations when the natural frequency was slightly higher than the vortex shedding frequency.[46]

In order to determine the relative merits of the two explanations for the high-frequency/low-Mach-number cutoff of the flutter boundary, Rainey's study of the problem[3] is consulted. One finds that the "sonic-tip-speed" criterion does not correlate the results whereas the cutoff around $\bar{\omega} \geq 2$ seems to occur. The flutter boundary obeys the relationship, $c\omega/a = 2.35\ M$, which is the same as saying that the high-frequency cutoff is $\bar{\omega} = 2.35$ ($c\omega/a = \bar{\omega} \times M$). Thus, it appears that the wake-resonance effect is best supported by experiments. It is also the criterion which has a physical explanation, usually a very important requisite for any mathematical model of a physical phenomenon. Stall flutter should again occur at frequen-

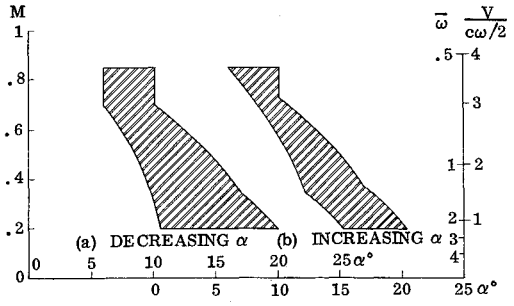

Fig. 13 Predicted stall-flutter boundaries for full-scale flight Reynolds numbers.

cies substantially higher than the wake frequency $\bar{\omega}$. The reason that this is not observed in reality could be that a dramatic reduction of the negative damping should occur for very high frequencies, $\bar{\omega} > 1$, when the phase lag of the deep stall characteristics exceeds 180°.[23]

In Fig. 13, the full-scale flutter boundaries predicted from static data for the NACA 64-012 airfoil are shown. The present analytic tools predict that the full-scale flutter boundary for the space shuttle transition maneuver, decreasing α, is the same as for the subscale wind-tunnel test, whereas the stall-flutter α-M region shrinks considerably for the case of increasing α. It should be emphasized that this insensitivity to flutter-test Reynolds number for decreasing α is caused by a saturation of dynamic improvements of the boundary layer due to the very high reduced frequencies associated with wing stall flutter. In the present analysis it is assumed that these viscous effects of the airfoil pitch rate dominate over the inviscid pressure-gradient effects. This insensitivity to Reynolds number has recently been observed in stall flutter tests of helicopter rotor blades.[47]

Conclusions

Several significant conclusions have been drawn from the results of this study of unsteady airfoil stall and stall flutter:

a) Stall flutter is caused by the negative aerodynamic damping generated at stall penetration. The α-boundaries for stall flutter are the highest and lowest angles of attack at which such a stall penetration loop can be established. For the large reduced frequencies associated with wing stall flutter, these upper and lower α-boundaries are shown to correspond to the static stall angles of attack in the limits of infinitely large and small Reynolds numbers.

b) For decreasing angle of attack through the stall region, as in the case of the space-shuttle transition maneuver, the true full-scale flutter boundaries will be measured in a subscale wind-tunnel test. These α-boundaries are predicted by the presented analysis, using experimental static data in combination with more or less routine corrections for compressibility effects.

c) The high-Mach-number/low-frequency cutoff of the stall-flutter region is purely an effect of Mach number. When the Mach number is increased beyond a certain critical value, the terminal shock is moving toward the trailing edge, and stall flutter will not result unless the elastic axis is far aft of the quarter chord.

d) The low-Mach-number/high-frequency cutoff of the stall-flutter region is shown to be the likely result of a resonance interaction between airfoil oscillation and Karman vortex shedding rather than the magical benefit of obtaining sonic differential sink velocities between leading and trailing edges ($c\omega/a \geq 1$).

Although the analysis is based on a series of approximations, and is of semiempirical nature, it is founded on realistic physical flow concepts and should provide a useful preliminary design tool. As formulated, the analysis will provide a conservative estimate; i.e., the predicted stall flutter region is slightly larger than the expected one, as demonstrated by comparison with experiments.

References

[1]Runyan, H. L. and Reed, W. H., "Dynamics and Aeroelasticity—An Appraisal," *Astronautics & Aeronautics,* Vol. 9, No. 2, Feb. 1971, pp. 48–57.

[2]Carta, F. O. and Niebanck, C. F., "Prediction of Rotor Instability at High Forward Speeds, Volume III, Stall Flutter," TR 68-18C, Feb. 1969, U.S. Army Aviation Material Labs., Fort Eustis, Va.

[3]Rainey, A. G., "Preliminary Study of Some Factors Which Affect the Stall-Flutter Characteristics of Thin Wings," TN 3622, 1956, NACA.

[4]Rainey, "Progress on the Launch Vehicle Buffeting Problem," *Journal of Spacecraft and Rockets,* Vol. 2, No. 3, May–June 1965, pp. 289–299.

[5]Ericsson, L. E. and Reding, J. P., "Analysis of Flow Separation Effects on the Dynamics of a Large Space Booster," *Journal of Spacecraft and Rockets,* Vol. 2, No. 4, July–Aug. 1965, pp. 481–490.

[6]Halfman, R. L., Johnson, H. C., and Haley, S. M., "Evaluation of High-Angle-of-Attack Aerodynamic-Derivative Data and Stall-Flutter Prediction Techniques," TN 2533, 1951, NACA.

[7]Liiva, J., Davenport, F. J., Gray, L., and Walton, I. C., "Two-Dimensional Tests of Airfoils Oscillating Near Stall," TR 68-13A & B, Apr. 1968, U.S. Army Aviation Material Labs., Fort Eustis, Va.

[8]Arcidiacono, P. J., Carta, F. O., Casellini, L. M., and Elman, H. L., "Investigation of Helicopter Control Loads Induced by Stall Flutter," TR 70-2, Mar. 1970, U.S. Army Aviation Material Labs., Fort Eustis, Va.

[9]Ham, N. D., "Stall Flutter of Helicopter Rotor Blades—A Special Case of the Dynamic Stall Phenomenon," *American Helicopter Society Journal,* Vol. 12, Oct. 1967, pp. 19–21.

[10]Ericsson, L. E. and Reding, J. P., "Dynamic Stall Simulation Problems," *Journal of Aircraft,* Vol. 8, No. 7, July 1971, pp. 579–583.

[11]Ham, N. D. and Garelick, M. S., "Dynamic Stall Considerations in Helicopter Rotors," *American Helicopter Society Journal,* Vol. 13, Apr. 1968, pp. 45–55.

[12]Ham, N. D. and Young, M. I., "Torsional Oscillation of Helicopter Blades Due to Stall," *Journal of Aircraft,* Vol. 3, No. 3, May–June 1966, pp. 218–224.

[13]McCroskey, W. J., and Fisher, R. K., Jr., "Detailed Aerodynamic Measurements on a Model rotor in the Blade Stall Regime," *American Helicopter Society Journal,* Vol. 17, Jan. 1972, pp. 20–30.

[14]Carta, F. O., "Effect of Unsteady Pressure Gradient Reduction on Dynamic Stall Delay," *Journal of Aircraft,* Vol. 8, Oct. 1971, pp. 839–841.

[15]Crimi, P. and Reeves, B. L., "A Method for Analyzing Dynamic Stall of Helicopter Rotor Blades," AIAA Paper 72-37, San Diego, Calif., 1972.

[16]Carta, F. O., Cassellini, L. M., Arcidiacono, P. J., and Elman, H. L., "Analytical Study of Helicopter Rotor Stall Flutter," *Proceedings of the American Helicopter Society, 26th Annual National Forum,* Preprint 413, 1970.

[17]Harris, F. D., Tarzanin, F. J., Jr., and Fisher, R. K., Jr., "Rotor High Speed Performance Theory vs. Test," *American Helicopter Society Journal,* Vol. 15, No. 3, July 1970, pp. 35–44.

[18]Tarzanin, F. J., "Prediction of Control Loads Due to Blade Stall," *Proceedings of the 27th Annual National V/STOL Forum,* Preprint 513, 1971.

[19]Ericsson, L. E., and Reding, J. P., "Unsteady Airfoil Stall, Review and Extension," *Journal of Aircraft,* Vol. 8, No. 8, Aug. 1971, pp. 609–616.

[20]Ericsson, L. E. and Reding, J. P., "Unsteady Airfoil Stall and Stall Flutter," CR-111906, June 1971, NASA.

[21]von Karman, Th. and Sears, W. R., "Airfoil Theory for Non-Uniform Motion," *Journal of Aeronautical Science,* Vol. 5, No. 10, Aug. 1938, pp. 379–390.

[22]Moore, F. K., "On the Separation of the Unsteady Laminar Boundary Layer," *Proceedings of the IUTAM Symposium on Boundary Layer Research,* 1957, pp. 296–311.

[23]Ericsson, L. E. and Reding, J. P., "Analytic Prediction of Dynamic Stall Characteristics," AIAA Paper 72-682, Boston, 1972.

[24]Gray, L., Liiva, J., and Davenport, F. J., "Wind Tunnel Tests of Thin Airfoils Oscillating Near Stall," TR 68-89A, Jan 1969, U.S. Army Aviation Material Labs., Fort Eustis, Va.

[25]Goetz, R. C., "Exploratory Study of Buffet and Stall Flutter of Space Shuttle Vehicle Wing Concepts," LWP-872, May 1970, NASA.

[26]Harper, P. W. and Flanigan, R. E., "The Effect of Rate of Change of Angle of Attack on the Maximum Lift of a Small Model," TN 2061, 1949, NACA.

[27]Wallis, R. A., "Boundary Layer Transition at the Leading Edge of Thin Wings and Its Effect on General Nose Separation," *Proceedings of the Second International Congress in the Aeronautical Sciences,* Vol. 3 1970, Institute of Aerospace Sciences, pp. 161–184.

[28]Schlichting, H., *Boundary Layer Theory,* McGraw-Hill, New York, 1955, pp. 206–213.

[29]Ericsson, L. E. and Reding, J. P., "Dynamic Stall of Helicopter Blades," *American Helicopter Society Journal,* Vol. 17, No. 1, Jan. 1972, pp. 10–19.

[30]Jacobs, E. N. and Sherman, A., "Airfoil Section Characteristics as Affected by Variations in the Reynolds Number," TR 586, 1937, NACA.

[31]Moss, G. F. and Murdin, P. M., "Two-Dimensional Low-Speed Tunnel Tests on the NACA 0012 Section Including Measurements Made During Pitch Oscillations at the Stall," C.P. No. 1145, Jan. 1970, Aeronautical Research Council, London, Great Britain.

[32]Gregory, N., Quincey, V. G., O'Reilly, C. L., and Hall, D. J., "Progress Report on Observations of Three-Deimensional Flow Patterns Obtained During Stall Development on Airfoils, and on the Problem of Measuring Two-Dimensional Characteristics," C.P. No. 1146, Jan. 1970, Aeronautical Research Council, London, Great Britain.

[33]Abbot, I. H., Von Doenhoff, A. E., and Stivers, L. S., "Summary of Airfoil Data," TR 824, 1945, NACA.

[34]Ville, G., "Influence des Decallements au Bord d'Attaque sur les Characteristiques Aerodynamiques des Voilures," *Proceedings of the 4th Colloque d'Aerodynamique Appliquee, Association Francaise des Ingenieurs et Techniciens des l'Aeronautique et de l'Espace,* 1967.

[35]Glauert, H., "The Effect of Compressibility on the Lift of Airfoils," *Proceedings of the Royal Society,* Series A, Vol. CXVIII, 1927, pp. 113–119.

[36]Harper, P. W. and Flanigan, R. E., "Investigation of the Variation of Maximum Lift for a Pitching Airplane Model and Comparison With Flight Results," TN 1734, 1948, NACA.

[37]Spreiter, J. R., Galster, G. M., and Blair, W. K., "Effect of Mach and Reynolds Number on the Maximum Lift Coefficient Obtainable in Gradual and Abrupt Stalls of a Pursuit Airplane Equipped With a Low Drag Wing," RM A5G06, 1945, NACA.

[38]Daley, B. N. and Lord, D. R., "Aerodynamic Characteristics of Several 6-Percent-Thick Airfoils at Angles of Attack From 0 to 20° at High Subsonic Speeds," TN 3424, 1955, NACA.

[39]Pearcey, H. H., "Some Effects of Shock-Induced Separation of Turbulent Boundary-Layers in Transonic Flow Past Airfoils," *Proceedings of the Symposium on Boundary Layer Effects in Aerodynamics,* Paper 9, National Physics Laboratory, Great Britain, 1955, pp. 1–84.

[40]Abbot, I. H. and von Doenhoff, A. E. *Theory of Wing Sections,* McGraw Hill, New York, 1949.

[41]Stengel, R. F., "Optimal Transition From Entry to Cruising Flight," *Journal of Spacecraft and Rockets,* Vol. 8, No. 11, Nov. 1971, pp. 1126–1132.

[42]Baker, J. E., "The Effects of Various Parameters, Including Mach Number, on Propeller-Blade Flutter With Emphasis on Stall Flutter," TN 3357, 1955, NACA.

[43]Woods, L. C., The Theory of Subsonic Plane Flow, *Cambridge University Press, 1961, pp. 45, 457, 475, 476,* Cambridge, Mass.

[44]Scruggs, R. M., "An Investigation of Near Wake Effects in Airtoil Dynamic Stall," Report 71-1, Mar. 1971, School of Aerospace Engineering, Georgia Inst. of Tech.

[45]Parkinson, G. V. and Ferguson, N., "Amplitude and Surface Pressure Measurements for a Circular Cylinder in Vortex-Excited Oscillation at Subcritical Reynolds Numbers," *Proceedings of the Meeting on Ground Wind Load Problems in Relation to Launch Vehicles,* Paper 18, NASA-Langley Research Center, 1966, pp. 18.1–18.12.

[46]Cincotta, J. J., Jones, G. W., and Walker, R. W., "Experimental Investigation of Wind-Induced Oscillation Effects on Cylinders in Two-Dimensional Flow at High Reynolds Numbers," *Proceedings of the Meeting on Ground Wind Load Problems in Relation to Launch Vehicles,* Paper 20, NASA-Langley Research Center, 1966, pp. 20.1–20.35.

[47]Benson, R. G., Dadone, L. U., Gormont, R. E., and Kohler, G. R. "Influence of Airfoils on Stall Flutter Boundaries of Articulated Helicopter Rotors," *Proceedings of the 28th Annual National V/STOL* Forum of the American Helicopter Society, Preprint 621, 1972.